

**Stereoselective Synthesis of Fluorinated Galactopyranosides as Potential  
Molecular Probes for Galactophilic Proteins: Assessment of  
Monofluorogalactoside–LecA Interactions**

Vincent Denavit,<sup>[a]</sup> Danny Lainé,<sup>[a]</sup> Chahrazed Bouzriba,<sup>[b, c]</sup> Elena Shanina,<sup>[d]</sup> Émilie  
Gillon,<sup>[e]</sup> Sébastien Fortin,<sup>[b, c]</sup> Christoph Rademacher,<sup>[d]</sup> Anne Imberty,<sup>[e]</sup> and Denis  
Giguère<sup>\*[a]</sup>

<sup>[a]</sup> *V. Denavit, D. Lainé, Prof. D. Giguère Département de Chimie, PROTEO, RQRM  
Université Laval, 1045 Avenue de la Médecine  
Quebec City, QC, G1V 0A6 (Canada)  
E-mail: [denis.giguere@chm.ulaval.ca](mailto:denis.giguere@chm.ulaval.ca)*

<sup>[b]</sup> *C. Bouzriba, Prof. S. Fortin  
Oncology Division, Hôpital Saint-François d'Assise  
CHU de Québec-Université Laval Research Center  
10 rue de l'Espinay, Quebec City, QC, G1L 3L5 (Canada)*

<sup>[c]</sup> *C. Bouzriba, Prof. S. Fortin  
Faculté de Pharmacie, Université Laval  
Quebec City, QC, G1V 0A6 (Canada)*

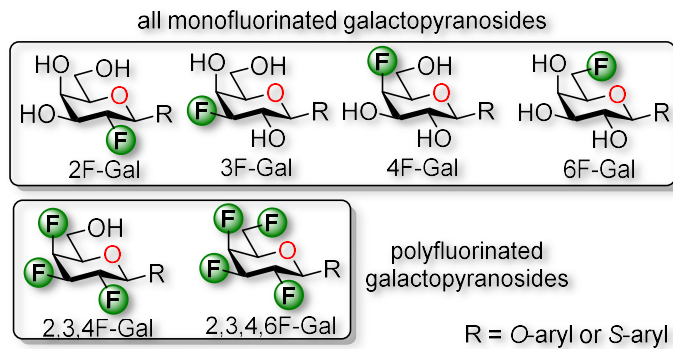
<sup>[d]</sup> *E. Shanina, Prof. C. Rademacher  
Department of Biomolecular Systems  
Max Planck Institute of Colloids and Interfaces  
Am Mühlenberg 1, 14424 Potsdam (Germany)*

[<sup>e</sup>] *P. Gillon, Prof. A. Imberty*

*Univ. Grenoble Alpes, CNRS, CERMAV*

*38000 Grenoble (France)*

### Graphical abstract



**Keywords:** carbohydrates, fluorinated glycoside, LecA, NMR spectroscopy, TROSY

NMR

## Abstract

The replacement of hydroxyl groups by fluorine atoms on hexopyranoside scaffolds may allow access to invaluable tools for studying various biochemical processes. As part of ongoing activities toward the preparation of fluorinated carbohydrates, a systematic investigation involving the synthesis and biological evaluation of a series of mono and polyfluorinated galactopyranosides is described. Various monofluorogalactopyranosides, a trifluorinated, and a tetrafluorinated galactopyranoside have been prepared using a Chiron approach. Given the scarcity of these compounds in the literature, in addition to their synthesis, their biological profiles were evaluated. Firstly, the fluorinated compounds were investigated as antiproliferative agents using normal human and mouse cells in comparison with cancerous cells. Most of the fluorinated compounds showed no antiproliferative activity. Secondly, these carbohydrate probes were used as potential inhibitors of galactophilic lectins. The first transverse relaxation-optimized spectroscopy (TROSY) NMR experiments were performed on these interactions, examining chemical shift perturbations of the backbone resonances of LecA, a virulence factor from *Pseudomonas aeruginosa*. Moreover, taking advantage of the fluorine atom, the  $^{19}\text{F}$  NMR resonances of the monofluorogalactopyranosides were directly monitored in the presence and absence of LecA to assess ligand binding. Lastly, these results were corroborated with the binding potencies of the monofluorinated galactopyranoside derivatives by isothermal titration calorimetry experiments. Analogues with fluorine atoms at C-3 and C-4 showed weaker affinities with LecA as compared to those with the fluorine atom at C-2 or C-6. This research has focused on the chemical synthesis of “drug-like” low-molecular-weight inhibitors that circumvent drawbacks typically associated with natural oligosaccharides.

## Introduction

The most widespread application of fluorinated carbohydrates is as radiopharmaceuticals for cancer imaging techniques.<sup>[1]</sup> Fluorinated carbohydrates are also invaluable tools as mechanistic probes to study lectin-carbohydrate interactions and to decipher the mechanisms of glycosidases.<sup>[2]</sup> To that end, deoxyfluoro sugars provide useful insights into the role of hydrogen-bonding interactions, allowing identification of the key active site(s) of enzyme-substrate interactions.

Lectins, carbohydrate-binding proteins, are found in all organisms from animals and plants to bacteria and viruses.<sup>[3]</sup> Lectins are involved in various biological processes, and their properties are related to their carbohydrate-binding domains.<sup>[4]</sup> Hence, it is crucial to elucidate and understand the sugar-binding properties of lectins.<sup>[5]</sup> Among them, galactose-specific lectins are of high interest as they bind, for example, to  $\beta$ -galactose present on branches of *N*-linked glycans, or to  $\alpha$ -galactose epitopes of some human and non-human blood groups.<sup>[6, 7]</sup> Galactose-specific lectins of therapeutic interest include LecA (PA-IL lectin from the pathogenic *Pseudomonas aeruginosa*), galectins, asialoglycoprotein receptor, and macrophage galactose-binding lectin. Extensive investigations have been devoted to understanding the ability of these lectins to regulate numerous biological processes. Since thorough understanding of biochemical pathways is hampered by the natural complexity of carbohydrates, chemical or chemo-enzymatic synthesis of glycomimetic ligands is likely to remain a valuable option in glycoscience. Therefore, there is a major need to develop new probes capable of targeting galactoside-specific lectins in order to decipher their binding characteristics.

The carbohydrate-binding capabilities of numerous lectins have been demonstrated by determining their abilities to bind glycan arrays and by inhibiting their interactions with glycoconjugates or glycomimetics.<sup>[8]</sup> This allows insight into the nature of the hydrogen bonding involved between the hydroxyl groups of carbohydrates and the binding sites of proteins. The monosaccharides used in these studies have generally included fluoro-, deoxy-, and thio-hexoses, along with uronic acids and alditols.<sup>[9]</sup> The major drawback associated with the use such diverse glycomimetic libraries is their poor synthetic availability. Consequently, the synthesis of fluoro-, deoxy-, and thio-glycosides is of high interest. In this context, we have sought to replace the hydroxyl groups of carbohydrates with fluorine atoms to generate new fluorine-substituted glycoside analogues.<sup>[10]</sup> The rationale for synthesizing such compounds stems from the similarity between the hydroxyl group and a fluoro substituent in terms of polarity and steric demand.<sup>[11]</sup> Also, the loss of hydrogen-donating capacity for the fluorine atom and the high C-F bond energy render them resistant to rapid in vivo degradation.<sup>[12]</sup> Finally, appending a fluoro substituent on a hydroxypyranose core can modulate the lipophilicity, which in turn can increase cell permeability.<sup>[13]</sup> Thus, fluorinated carbohydrates can be considered as more “drug-like” tools that circumvent drawbacks typically associated with natural oligosaccharides, such as low affinity, limited metabolic stability, and high polarity leading to low bioavailability.

As part of our ongoing program related to the synthesis of fluorinated carbohydrates,<sup>[14]</sup> our attention was turned toward the preparation of monofluorogalactopyranosides **1-4**, along with the tetrafluorinated galactopyranoside congener **6** (Figure 1). On our way to preparing the polyfluoro derivative, we were also able to access trifluorinated galactopyranoside **5**. Heavily fluorinated hexopyranosides (replacement of multiple

hydroxyl groups by fluorine atoms) are particularly interesting because of the synthetic challenge they present. We have developed convenient synthetic methodologies to enable further biological investigations. In order to increase the molecular diversity of our library, two aglycones were installed at the anomeric position, a  $\beta$ -*O*-benzoic acid and a  $\beta$ -*S*-(2-naphthyl) moiety, since some galactoside-specific lectins are known to bind to such structural motifs.<sup>[15]</sup>

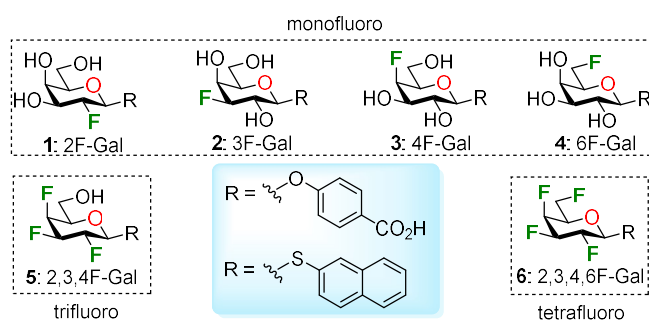


**Figure 1.** Mono- and polyfluorinated galactopyranosides prepared in this work.

In the context of this study, it is important to point out that heavily fluorinated carbohydrates have hitherto only been used in kinetic studies,<sup>[16]</sup> to improve protein-carbohydrate interactions,<sup>[17]</sup> in the development of chemically modified analogues with improved antigenicity,<sup>[18]</sup> and in studies of their ability to cross erythrocyte membranes.<sup>[19]</sup> The interesting properties of polyfluorinated carbohydrates can partly be explained in terms of a desolvation effect, together with attractive dipolar interactions mediated by polar C-F bonds.<sup>[20]</sup> Herein, we present the first library and biological investigation of synthetic monofluorinated galactopyranosides. To the best of our knowledge, only one report has described the hydrolysis of a series of fluorogalactopyranosides.<sup>[21]</sup> However, the synthetic preparation of these compounds was not described. Herein, we disclose the first

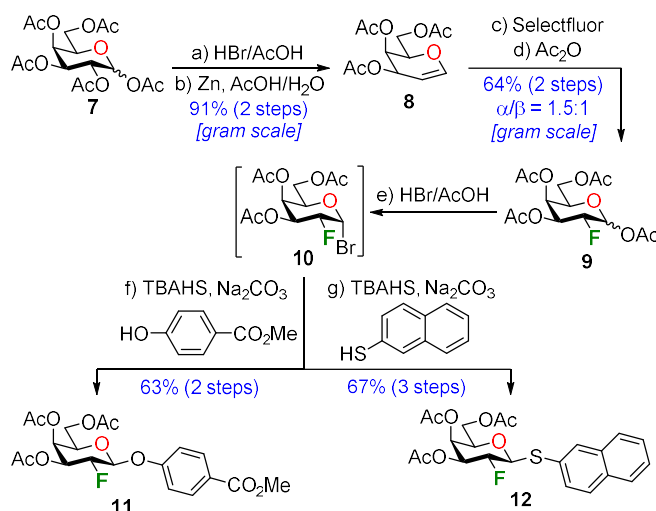
antiproliferative screening of mono- and polyfluorinated galactopyranosides toward human HaCat primary epidermal keratinocyte, human HDFn neonatal dermal fibroblast, and mouse 3T3 embryonic fibroblast normal cells. The results were compared with those towards human HT-29 colon adenocarcinoma and human M21 skin melanoma cancer cells. The compounds of our synthetic library could also be useful as stable molecular probes for galactophilic lectins. This is exemplified by the first TROSY NMR monitoring of the chemical shift perturbation of LecA from the virulence factor *Pseudomonas aeruginosa*. Moreover, taking advantage of the properties of the fluorine atom, direct detection of the  $^{19}\text{F}$  NMR resonances of monofluorogalactopyranosides in the presence of LecA has been carried out to identify chemical shift changes of the ligands. Finally, these results were corroborated by determining the binding potencies of the monofluorinated galactopyranoside derivatives by isothermal titration calorimetry.

## Results and Discussion

Our synthetic endeavors started with the preparation of 2-fluorogalactopyranosides. Compounds such as 2F-glycosides are important tools, used as specific mechanism-based glycosidase inhibitors.<sup>[16a, 22]</sup> The synthesis of 2-deoxy-2-fluoro-galactopyranoside derivatives is summarized in Scheme 1. Thus, acetylated galactoside **7** was transformed in two steps into known 2,3,6-tri-*O*-d-galactal **8** in 91% yield. Treatment of compound **8** with SelectfluorS on a large scale led exclusively to 2-deoxy-2-fluorod-galactopyranoside **9** after *O*-acetyl protection of the anomeric position ( $\alpha/\beta=1.5:1$ ).<sup>[23]</sup> Stereoselective installation of the anomeric aglycone proceeded through the  $\alpha$ -galactosyl bromide **10**. The crude bromide product underwent a phase-transfer-catalyzed nucleophilic displacement

with methyl 4-hydroxybenzoate or 2-naphthalenethiol, leading to derivatives **11** (63% yield over two steps) and **12** (55% yield over two steps), respectively. The  $\beta$  configurations were determined from direct NMR couplings between the anomeric proton and the H-2 proton and the fluorine atom at C-2 [ $^1\text{H}$  NMR (500 MHz):  $\delta=5.23$  (dd,  $^3J_{\text{H1-H2}}=7.4$  Hz,  $^3J_{\text{H1-F2}}=3.8$  Hz) for **11** and  $\delta=4.82$  (dd,  $^3J_{\text{H1-H2}}=9.6$  Hz,  $^3J_{\text{H1-F2}}=2.8$  Hz) for **12**]. This methodology was applied for determination of the anomeric configurations of all of the galactopyranoside derivatives prepared in this study.<sup>[24]</sup>

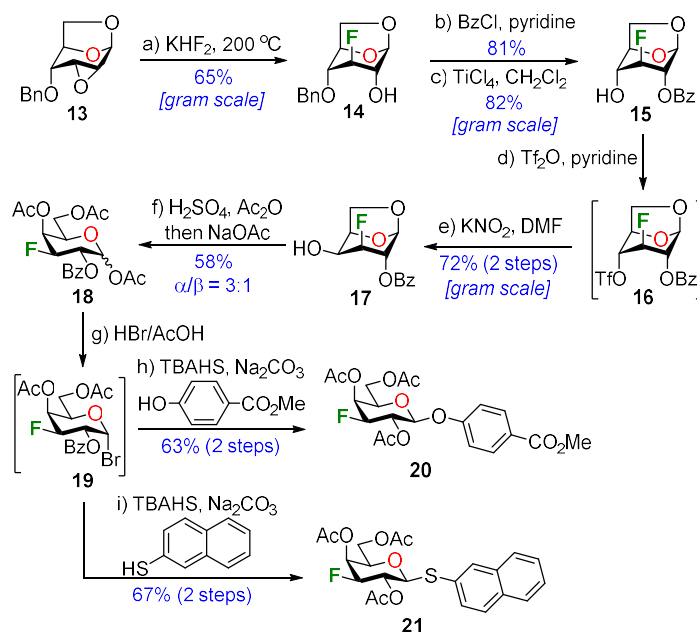




**Scheme 1.** Synthesis of 2-deoxy-2-fluorogalactopyranosides **11** and **12**. a) HBr/AcOH, CH<sub>2</sub>Cl<sub>2</sub>, rt, 2 h; b) Zinc (5.3 equiv), AcOH/H<sub>2</sub>O (4/1), rt, 5 h, 91% over 2 steps; c) Selectfluor<sup>®</sup> (1.2 equiv), CH<sub>3</sub>NO<sub>2</sub>/H<sub>2</sub>O (5/1), rt, 18 h; d) Ac<sub>2</sub>O/pyridine (1/5), rt, 20 h, 64% over 2 steps; e) HBr/AcOH, CH<sub>2</sub>Cl<sub>2</sub>, rt, 42 h; f) methyl 4-hydroxybenzoate (3.0 equiv), TBAHS (1.0 equiv.), AcOEt/1M Na<sub>2</sub>CO<sub>3</sub> (1/1), rt, 18 h, 63% over 2 steps; g) 2-thionaphthyl (3.0 equiv), TBAHS (1.0 equiv.), AcOEt/1M Na<sub>2</sub>CO<sub>3</sub> (1/1), rt, 18 h, 55% over 2 steps. AcOH = acetic acid, Ac<sub>2</sub>O = acetic anhydride, Selectfluor = 1-chloromethyl-4-fluoro-1,4-diazoniabicyclo[2.2.2]octane bis(tetrafluoroborate); TBAHS = tetrabutylammonium hydrogen sulfate.

Our next challenge was the preparation of 3-deoxy-3-fluorogalactopyranoside derivatives, which was based on our previously described method and summarized in Scheme 2.<sup>[14b]</sup> Briefly, Cerny's epoxide **13**<sup>[25]</sup> was treated with potassium hydrogen fluoride in ethylene glycol at 200 °C for 5 h to afford the desired 3-deoxy-3-fluoroglucopyranose **14** in 65% yield as the sole isomer. With the required 3-deoxy-3-fluoro derivative in hand, the next task was inversion of configuration at C-4. Thus, benzylation of the free hydroxyl group

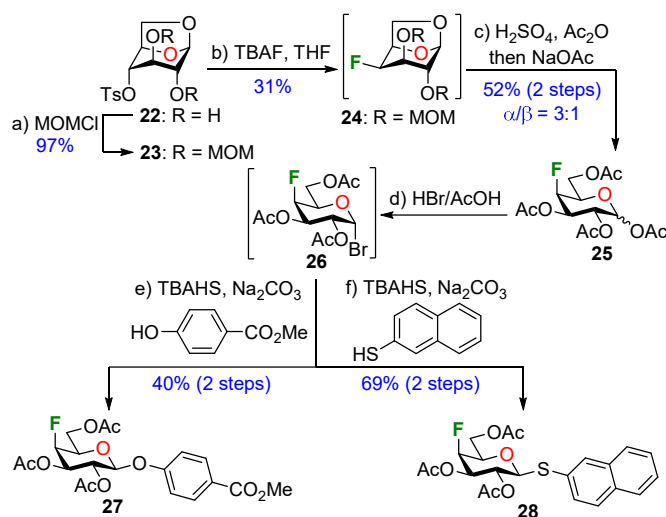
was followed by deprotection of the 4-*O*-benzyl group using TiCl<sub>4</sub>. Compound **15** was then subjected to Lattrell-Dax epimerization on a gram scale through formation of triflate **16**.<sup>[26]</sup> The crude mixture was treated with KNO<sub>2</sub> in DMF to generate the desired 1,6-anhydro-β-D-galactopyranose derivative **17** in 72% yield over two steps. Acetolysis using a mixture of H<sub>2</sub>SO<sub>4</sub> and Ac<sub>2</sub>O allowed the generation of protected 3-deoxy-3-fluoro-D-galactopyranose **18** in 58% yield (a/b=3:1). Stereoselective functionalization of the anomeric position was easily achieved as described above. Thus, treatment with HBr/AcOH generated bromide **19**, which could then be subjected to the phase-transfer-catalyzed reaction. Methyl 4-hydroxybenzoate **20** and 2-naphthalenethiol **21** were isolated in yields of 63% and 67%, respectively, over two steps.



**Scheme 2.** Synthesis of 3-deoxy-3-fluorogalactopyranosides **20** and **21**. a)  $\text{KHF}_2$  (6.1 equiv), ethylene glycol, 200 °C, 5 h, 65%; b)  $\text{BzCl}$  (3.0 equiv), pyridine,  $\text{CH}_2\text{Cl}_2$ , rt, 1 h, 81%; c)  $\text{TiCl}_4$  (1.1 equiv),  $\text{CH}_2\text{Cl}_2$ , 0 °C, 1 h, 82%; d)  $\text{Tf}_2\text{O}$  (2.3 equiv), pyridine,  $\text{CH}_2\text{Cl}_2$ , 0 °C to rt, 0.5 h; e)  $\text{KNO}_2$  (3.0 equiv), DMF, rt, 24 h, 72% over 2 steps; f)  $\text{H}_2\text{SO}_4$  (10 equiv),  $\text{Ac}_2\text{O}$  (30 equiv), rt, 18 h, then  $\text{NaOAc}$  (20 equiv), rt, 0.3 h, 58% ( $\alpha/\beta = 3:1$ ); g)  $\text{HBr}/\text{AcOH}$ ,  $\text{CH}_2\text{Cl}_2$ , 0 °C to rt, 2 h; h) methyl 4-hydroxybenzoate (3.0 equiv), TBAHS (1.0 equiv),  $\text{AcOEt}/1\text{M Na}_2\text{CO}_3$  (1/1), rt, 18 h, 63% over 2 steps; i) 2-thionaphthyl (3.0 equiv), TBAHS (1.0 equiv),  $\text{AcOEt}/1\text{M Na}_2\text{CO}_3$  (1/1), rt, 18 h, 67% over 2 steps.  $\text{Ac}_2\text{O}$  = acetic anhydride,  $\text{BzCl}$  = benzoyl chloride, DMF = *N,N*-dimethylformamide,  $\text{NaOAc}$  = sodium acetate, TBAHS = tetrabutylammonium hydrogen sulfate,  $\text{Tf}_2\text{O}$  = trifluoromethanesulfonic anhydride.

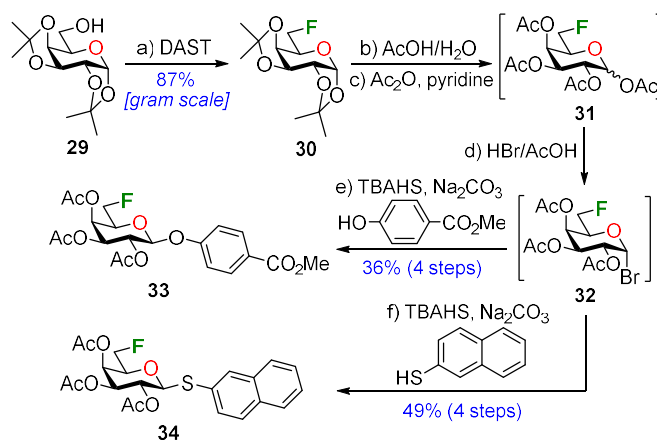
The syntheses of 4-deoxy-4-fluoro-galactopyranoside derivatives started from the known 4-*O*-*p*-toluenesulfonyl derivative **22** (Scheme 3).<sup>[27]</sup> Protection of the residual hydroxyl

group allowed the preparation of compound **23** in high yield, which was subjected to nucleophilic fluorination using TBAF in boiling THF. Compound **24** was isolated together with an unidentifiable impurity, and was directly subjected to acetolysis under acidic conditions. The concomitant removal of the MOM protecting group proceeded as expected, generating intermediate **25** in 52% yield over two steps ( $\alpha/\beta=3:1$ ).<sup>[16c]</sup> Finally, the anomeric groups were installed as described above, allowing the isolation of products **27** and **28** via bromide intermediate **26**.



**Scheme 3.** Synthesis of 4-deoxy-4-fluorogalactopyranoside **27** and **28**. a) MOMCl (10 equiv), DIPEA (11 equiv), CH<sub>2</sub>Cl<sub>2</sub>, 40 °C, 18 h, 97%; b) TBAF (10 equiv), THF, 66 °C, 72 h, 31%, based on 76% purity; c) H<sub>2</sub>SO<sub>4</sub> (10 equiv), Ac<sub>2</sub>O (30 equiv), rt, 18 h; then NaOAc (20 equiv), rt, 0.3 h, 52 % over 2 steps,  $\alpha/\beta = 4:1$ ; d) HBr/AcOH, CH<sub>2</sub>Cl<sub>2</sub>, rt, 1 h; e) methyl 4-hydroxybenzoate (3.0 equiv), TBAHS (1.0 equiv), AcOEt/1M Na<sub>2</sub>CO<sub>3</sub> (1/1), rt, 18 h, 40% over 2 steps; f) 2-thionaphthyl (3.0 equiv), TBAHS (1.0 equiv), AcOEt/1M Na<sub>2</sub>CO<sub>3</sub> (1/1), rt, 18 h, 69% over 2 steps. Ac<sub>2</sub>O = acetic anhydride, DIPEA = *N,N*-diisopropylethylamine, MOMCl = chloromethyl methyl ether, NaOAc = sodium acetate, TBAF = tetrabutylammonium fluoride, TBAHS = tetrabutylammonium hydrogen sulfate.

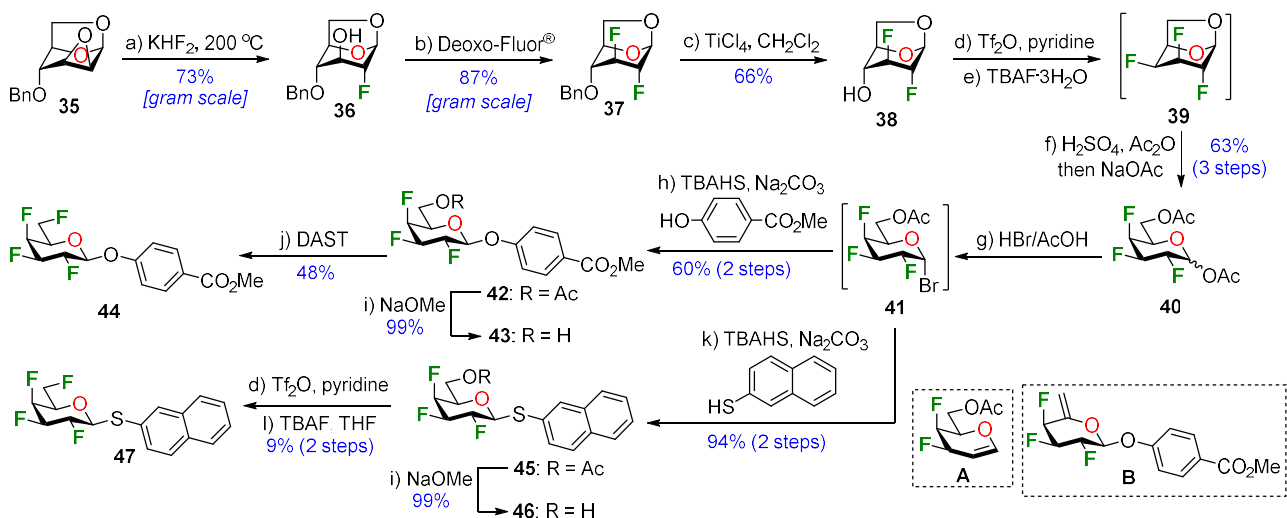
The most conveniently prepared fluorinated analogue was undoubtedly the 6-deoxy-6-fluoro-galactopyranose. The synthetic route was straightforward and commenced from 1,2:3,4-di-*O*-isopropylidene- $\alpha$ -D-galactopyranose **29**, an inexpensive starting material (Scheme 4). Fluoro derivative **30** was isolated in 87% yield by treatment with Me-DAST under microwave irradiation (80 °C) for 1 h. This method provided a higher yield as compared to conventional heating.<sup>[14b]</sup> Isopropylidene hydrolysis was followed by acetyl protection, furnishing an anomeric mixture of 6-deoxy-6-fluoro-galactopyranose **31**. The latter was subjected to acidic conditions followed by phase-transfer-catalyzed reaction. Product **33** was isolated in 36% yield over four steps (78% per step) and product **34** was isolated in 49% yield over four steps (83% per step).



**Scheme 4.** Synthesis of 6-deoxy-6-fluorogalactopyranoside **33** and **34**. a) DAST (1.2 equiv), 2,4,6-collidine (2.4 equiv),  $\text{CH}_2\text{Cl}_2$ , 80 °C, microwave irradiation, 1 h, 87 %; b) AcOH/ $\text{H}_2\text{O}$  (4:1), reflux, 18 h; c)  $\text{Ac}_2\text{O}$ , pyridine, rt, 72 h; d) HBr/AcOH,  $\text{CH}_2\text{Cl}_2$ , rt, 2 h; e) methyl 4-hydroxybenzoate (3.0 equiv), TBAHS (1.0 equiv), AcOEt/1M  $\text{Na}_2\text{CO}_3$  (1/1), rt, 18 h, 36% over 4 steps; f) 2-thionaphthyl (3.0 equiv), TBAHS (1.0 equiv), AcOEt/1M  $\text{Na}_2\text{CO}_3$  (1/1), rt, 18 h, 49% over 4 steps. AcOH = acetic acid,  $\text{Ac}_2\text{O}$  = acetic anhydride, DAST = diethylaminosulfurtrifluoride, TBAHS = tetrabutylammonium hydrogen sulfate.

In order to increase the molecular diversity of our library, our next aim was the preparation of tetrafluorinated galacto pyranosides.<sup>[14a]</sup> Along the way, it became obvious that we could also access one trifluorinated galactopyranoside. Our synthetic endeavors toward this end are depicted in Scheme 5 and start with easily accessible Cerny's epoxide **35**, which was obtained in four steps from levoglucosan.<sup>[28]</sup> Nucleophilic fluorination of the 2,3-anhydro derivative **35** was achieved in 73% yield by treatment with potassium hydrogen fluoride. Treatment of **36** with Deoxo-Fluor<sup>®</sup> furnished 2,3-dideoxy-difluoroglucose **37** in high yield with complete retention of configuration. This result can be explained in terms of a trans-diaxially positioned benzyloxy group at C-4 capable of participation through an

oxiranium intermediate species<sup>[29]</sup> TiCl<sub>4</sub>-mediated benzyl deprotection furnished compound **38** in 66% yield, which was the ideal precursor to generate the 1,6-anhydro 2,3,4-trideoxy-trifluoro-β-D-galactopyranose **39**. Thus, the free *O*-4 hydroxyl group on compound **38** was activated as a triflate and subjected to nucleophilic fluorination with TBAF to afford compound **39** with complete inversion of configuration. Isolation and purification of trifluoro-sugar **39** proved to be difficult due to its high volatility. Consequently, the crude mixture was subjected to acidic conditions (H<sub>2</sub>SO<sub>4</sub>, Ac<sub>2</sub>O), generating the acetolysis product **40** in 63% yield over three steps.<sup>[30]</sup> The configurations of the fluoro substituents were ascertained on the basis of <sup>19</sup>F NMR spectroscopy [<sup>19</sup>F NMR (470 MHz): <sup>3</sup>J<sub>F<sub>2</sub>-H<sub>3</sub></sub>=12.8 Hz, <sup>3</sup>J<sub>F<sub>3</sub>-F<sub>4</sub></sub>=13.4 Hz, <sup>3</sup>J<sub>F<sub>3</sub>-H<sub>4</sub></sub>=6.4 Hz, <sup>3</sup>J<sub>F<sub>4</sub>-H<sub>3</sub></sub>=<sup>3</sup>J<sub>F<sub>4</sub>-H<sub>5</sub></sub>=27.0 Hz]. The aglycones were installed using the same strategy as described above, affording compounds **42** and **45** via bromide **41**. In both reactions, side product A was isolated from the mixture, originating from elimination of the anomeric bromo substituent (Scheme 5). The last task was deoxofluorination at C-6, which proved to be more challenging than expected.<sup>[14a]</sup> Following extensive experimentation, it was found that DAST-mediated deoxofluorination of **43** afforded polyfluorohexopyranose **44** in 57% yield (together with 32% of the 1-arabinohex-5-enopyranoside derivative **B**). For compound **45**, due to the instability of the thionaphthyl moiety under the deoxofluorination conditions,<sup>[31]</sup> a different approach had to be followed. When the free hydroxyl group of **46** was activated as a triflate after de-*O*-acetylation, nucleophilic fluorination using TBAF gave a disappointing 9% yield. Instead, elimination of the C-6 leaving group led to derivative C in 83% yield. This example clearly shows the limitation of deoxyfluorination of aryl thiohexopyranoside analogues.



**Scheme 5.** Synthesis of trifluorinated **43** and **46** and tetrafluorinated **44** and **47** galactopyranoside derivatives. a)  $\text{KHF}_2$  (7.0 equiv), ethylene glycol, 200 °C, 2.5 h, 73%; b) Deoxofluor<sup>®</sup> (2.0 equiv), THF, microwave irradiation, 100 °C, 1.5 h, 87%; c)  $\text{TiCl}_4$  (1.1 equiv),  $\text{CH}_2\text{Cl}_2$ , 0 °C, 0.5 h, 66%; d)  $\text{Tf}_2\text{O}$  (2.0 equiv), pyridine (3.0 equiv), 0 °C, 0.2 h; e) TBAF·3 $\text{H}_2\text{O}$  (1.5 equiv),  $\text{CH}_2\text{Cl}_2$ , rt, 15 h; f)  $\text{Ac}_2\text{O}$  (30 equiv),  $\text{H}_2\text{SO}_4$  (10 equiv), 0 °C to rt, 18 h, then NaOAc (20 equiv), rt, 0.3 h, 63% over 3 steps,  $\alpha/\beta = 5:1$ ; g) 33% HBr in AcOH,  $\text{CH}_2\text{Cl}_2$ , rt, 66 h; h) methyl *p*-hydroxybenzoate (3.0 equiv), TBAHS (1.0 equiv.), EtOAc, 1M  $\text{Na}_2\text{CO}_3$ , rt, 18 h; 60% over 2 steps; i) 1M NaOMe, MeOH, rt, 1 h, 99% for **43**, 99% for **46**; j) DAST (3.0 equiv), 2,4,6-collidine (6.0 equiv),  $\text{CH}_2\text{Cl}_2$ , microwave irradiation, 100 °C, 1 h, 48%; k) 2-thionaphthyl (3.0 equiv), TBAHS (1.0 equiv), EtOAc, 1M  $\text{Na}_2\text{CO}_3$ , rt, 18 h; 94% over 2 steps; l)  $\text{Tf}_2\text{O}$  (2.0 equiv), pyridine (10.0 equiv), 0 °C, 0.5 h; m) 1M TBAF in THF (15 equiv), -78 °C to rt, 15 h, 9% over 2 steps.  $\text{Ac}_2\text{O}$  = acetic anhydride, DAST = diethylaminosulfurtrifluoride, Deoxofluor = *bis*(2-methoxyethyl)aminosulfurtrifluoride, TBAF = tetrabutylammonium fluoride, TBAHS = tetrabutylammonium hydrogen sulfate,  $\text{Tf}_2\text{O}$  = trifluoromethanesulfonic anhydride.



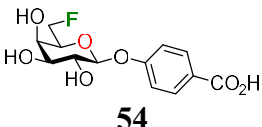
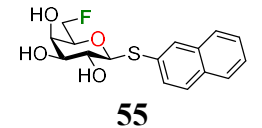
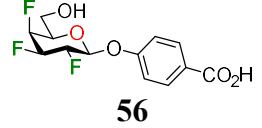
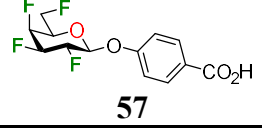
Complete deprotection of our target products was achieved according to two distinct protocols, depending on the substrate (Table 1). In the case of the methyl *p*-(*O*-galactosyl)benzoate analogues, lithium hydroxide was used for concomitant de-*O*-acetylation and generation of the acid moiety, furnishing compounds **48**, **50**, **52**, **54**, **56**, and **57**. For thiogalactoside analogues, a classical Zemplén de-*O*-acetylation (NaOMe, MeOH) provided the desired products **49**, **51**, **53**, and **55**. Both methods furnished clean products in high yields.

**Table 1.** Deprotection of acetylated fluorogalactopyranosides generating analogs **48-57**.

Method A: LiOH  
or  
Method B: NaOMe

R = OAc or F  
X = O or S

Entry	Starting material	Method <sup>a</sup>	Product	Yield (%) <sup>b</sup>
1	<b>11</b>	A		89
2	<b>12</b>	B		97
3	<b>20</b>	A		92
4	<b>21</b>	B		98
5	<b>27</b>	A		86
6	<b>28</b>	B		94

7	<b>33</b>	A	 <b>54</b>	93
8	<b>34</b>	B	 <b>55</b>	98
9	<b>43</b>	A	 <b>56</b>	94
10	<b>44</b>	B	 <b>57</b>	97

<sup>a</sup>Method A: 1M LiOH (3.5 equiv), H<sub>2</sub>O/MeOH/THF (2:3:5); Method B: NaOMe in MeOH.

<sup>b</sup>Yields refer to isolated pure products

To extend this study, we investigated key physical properties of some of our fluorinated carbohydrates. Firstly, in order to unambiguously establish the configuration of the fluoro substituents of the polyfluorinated galactopyranoside derivatives, the X-ray crystal structure of **57** was determined (Figure 2).<sup>[32]</sup> We identified a crystalline polymorph with a different space group to that reported previously.<sup>[14a, 33]</sup> In the solid state, compound **57** exists as a dimer, and the hexopyranose ring adopts a <sup>4</sup>C<sub>1</sub> conformation. Secondly, we compared the <sup>19</sup>F NMR spectra of compounds **48**, **50**, **52**, **54**, **56**, and **57** (Figure 3). The assessment of coupling constants in <sup>19</sup>F and <sup>1</sup>H NMR represents a reliable approach for determining the absolute configurations and conformations of fluorinated carbohydrates. Figure 3 shows that the multiplicities are very consistent, and depend on the relative spatial relationships between neighboring atoms. Each of the fluorinated carbohydrates adopts the <sup>4</sup>C<sub>1</sub> conformation. For polyfluorinated analogues **56** and **57**, comparison of the fluorine signals with those of the monofluorinated counterparts reveals that the F-H coupling

constants are similar, despite a slight change in chemical shift. Finally, the C-6 fluoro substituent in compound **54** adopts either a transgauche (TG) or gauche-trans (GT) conformation. This was confirmed by analysis of the  $^1\text{H}$  NMR spectrum (500 MHz). The proton at C-5 has a chemical shift of  $\delta=4.02$  ppm with, amongst others, a coupling constant of  $^3J_{\text{H5-F6}}=15.2$  Hz, corresponding to a gauche conformation with respect to F-6. A similar result was obtained for compound **57** (H-5:  $\delta=4.52$  ppm with  $^3J_{\text{H5-F6}}=12.9$  Hz). This result is at variance with the conformation of the fluoro substituent at C-6 of compound **57** in the solid state (Figure 2). The gauche-gauche (GG) conformer, corresponding to the crystal structure, represents one of the highest-energy conformations.<sup>[14a, 34]</sup> Our experiments confirmed  $^{19}\text{F}$  NMR to be an invaluable tool for analyzing the structural conformations of such organofluorine compounds.

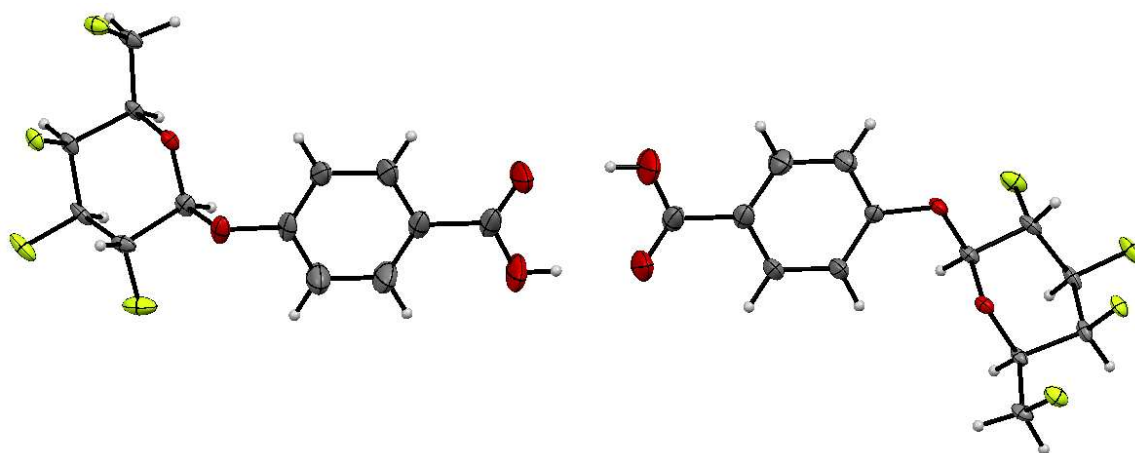


**Figure 2.** X-ray crystallographic analysis-derived ORTEP of **57** showing 50% thermal ellipsoid probability; carbon (grey), oxygen (red), fluorine (light-green), hydrogen (white).

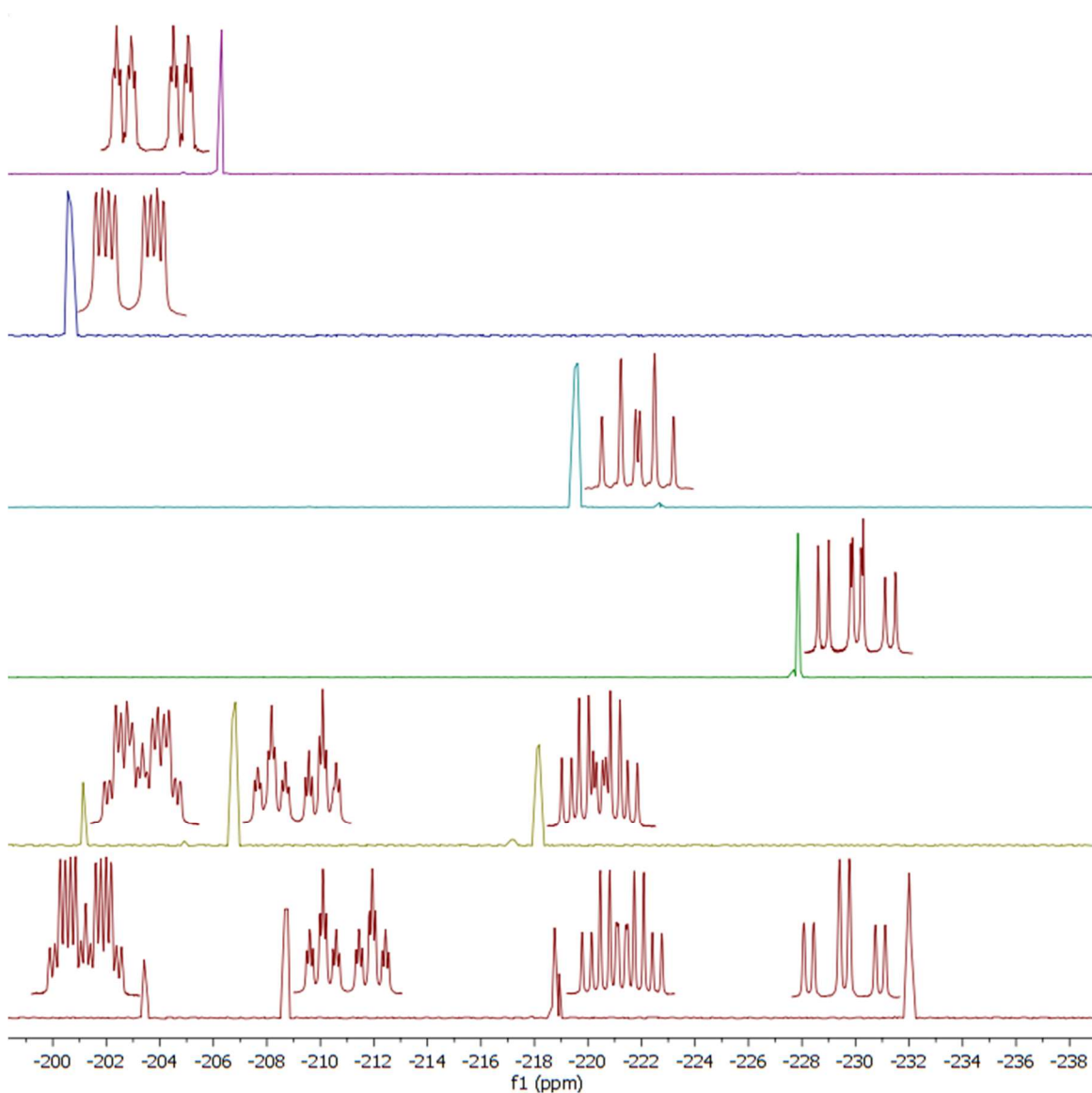


**Figure 3.** Direct comparison of  $^{19}\text{F}$  resonances of compounds **48**, **50**, **52**, **54**, **56**, and **57** ( $^{19}\text{F}$  NMR, 470 MHz). Expansions of the spectra display the coupling constants of each signal.

### Antiproliferative activity

We wished to use our library of fluorinated galactopyranosides in various biological systems, and thus evaluated their antiproliferative profiles. Compounds **43**, **46**, and **48-56**

were tested for their antiproliferative activities against human HaCaT primary epidermal keratinocyte, human HDFn neonatal dermal fibroblast, and mouse 3T3 embryonic fibroblast normal cells, as compared with those against human HT-29 colon adenocarcinoma and human M21 skin melanoma cancer cells (Table 2).

**Table 2.** Antiproliferative activity ( $IC_{50}$ ) of molecular probe (**48–56**) derivatives on human HaCaT primary epidermal keratinocyte, human HDFn neonatal dermal fibroblast and mouse 3T3 embryonic fibroblast normal cells as compared with human HT-29 colon adenocarcinoma and human M21 skin melanoma cancer cells.

Compounds	$IC_{50}$ ( $\mu M$ ) <sup>a</sup>				
	Normal cell lines			Cancer cell lines	
	HaCaT	HDFn	3T3	HT-29	M21
<b>43</b>	> 100	> 100	> 100	> 100	> 100
<b>46</b>	69	45	56	38	34
<b>48–56</b>	> 100	> 100	> 100	> 100	> 100
<b>Topotecan</b>	0.18	0.24	0.48	0.34	2.0

<sup>a</sup> $IC_{50}$  is expressed as the concentration of drug inhibiting cell proliferation by 50% after 48 h of treatment.

Most of the fluorinated compounds (**43** and **48–56**) showed no antiproliferative activity against normal or cancer cell lines and could therefore be used in various cell assays. In contrast, trifluorinated galactose derivative **46** bearing a thionaphthyl moiety showed some activity, with no selectivity towards normal cell lines ( $IC_{50}$ =45-69  $\mu M$ ) and cancer cell lines ( $IC_{50}$ =34-38  $\mu M$ ). Thus, **46** is a weak antiproliferative agent compared to Topotecan, a known chemotherapeutically active compound.

## Biophysical measurements

*Pseudomonas aeruginosa* is a Gram-negative bacterium and a leading pathogen for infections of immune-compromised patients and patients suffering from cystic fibrosis.<sup>[35]</sup> LecA is a virulence factor crucial for biofilm formation by *P. aeruginosa* and has been demonstrated to be involved in adhesion to lung tissues.<sup>[36]</sup> This lectin shows a strong specificity for  $\alpha$ -galactopyranose-terminated oligosaccharides, although  $\beta$ -galactopyranosides possessing an aromatic aglycon have been reported to be efficient binders.<sup>[15b, 37]</sup> Moreover, 2-naphthyl-1-thio- $\beta$ -D-galactopyranoside has been reported to show high affinity for LecA ( $K_D=6.3 \mu\text{M}$ ), an affinity increase nicely supported by the available X-ray crystal structure of its binding with the lectin (PDB code 3ZYF).<sup>[15b]</sup> In the context of this study, we envisaged that our library of fluorinated galactosides could represent efficient synthetic glycomimetics of natural  $\alpha$ -linked oligosaccharides with improved properties. To unveil such interactions, we first examined chemical shift perturbations in  $^1\text{H}$ ,  $^{15}\text{N}$ -TROSY (transverse relaxation-optimized spectroscopy) spectra of the backbone amide resonances of  $^{15}\text{N}$ -labelled LecA induced by interactions with our fluorinated probes. To the best of our knowledge, these are the first TROSY NMR experiments on LecA, and this milestone could be useful for future related experiments. Complementary to these studies, we followed the perturbations of the isolated and sensitive  $^{19}\text{F}$  resonances of the compounds. Finally, the results of these NMR experiments were corroborated through isothermal titration calorimetry experiments.

The  $^1\text{H}$ ,  $^{15}\text{N}$ -TROSY NMR spectra of our probes bound to  $^{15}\text{N}$ -labelled LecA clearly demonstrated that the position of the fluoro substituent on the pyranose ring strongly

influences the binding of galactose to the protein. This is exemplified in Figure 4a by the spectra of  $^{15}\text{N}$ -labelled LecA in the presence (orange) and absence (blue) of 2-deoxy-2-fluoro-galactopyranoside **48**. Multiple perturbations of backbone chemical shifts and line broadening of these resonances were visible, particularly relating to the amino acids constituting the carbohydrate recognition domain, as inferred from experiments with unsubstituted galactose. In contrast, 4-deoxy-4-fluoro-galactopyranoside **52** induced significantly less pronounced perturbations in the protein backbone, indicative of a reduced interaction (Figure **4b**). Clearly, the fluoro substituent at C-4 abrogates binding to LecA.

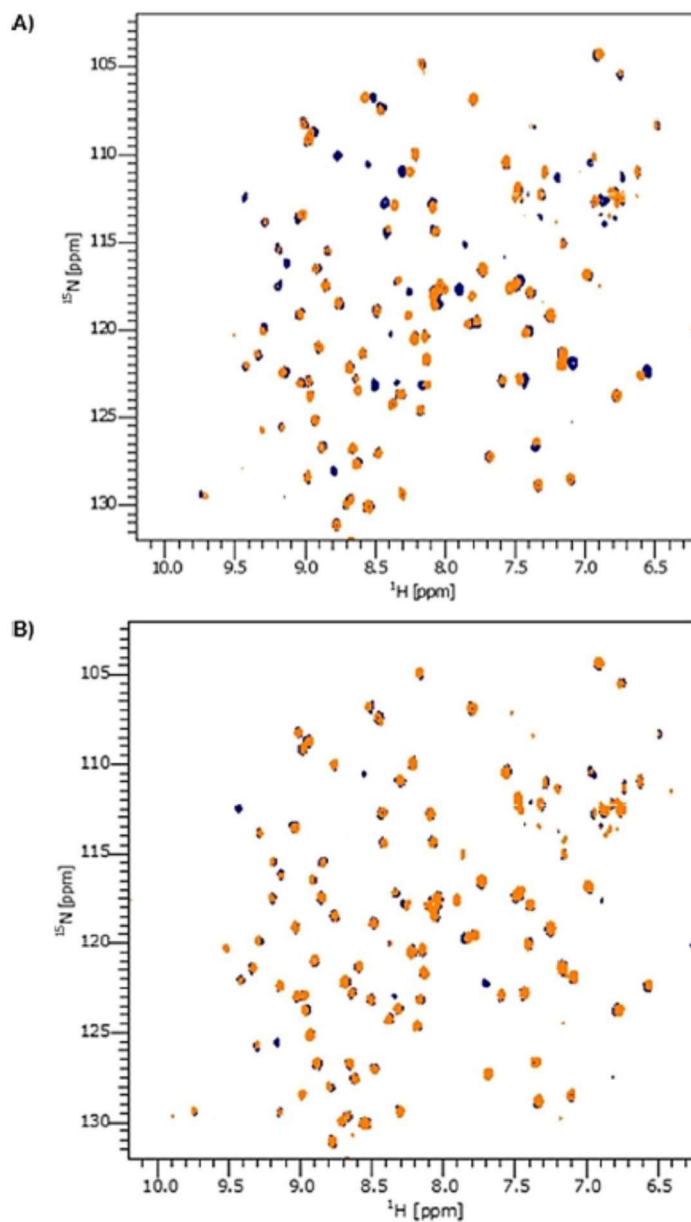


**Figure 4.** Chemical shift perturbations of backbone resonances of LecA upon binding to galactose derivatives **48** and **52** as observed in  $^1\text{H},^{15}\text{N}$ -TROSY NMR experiments. Spectra of 350  $\mu\text{M}$   $^{15}\text{N}$ -labelled LecA in the absence (blue) and presence (orange) of monofluorinated galactoside are shown for A) 0.2 mM **48** and B) 1.0 mM **52**. Fluorination at C2 (**48**) induces multiple chemical shift perturbations and line broadening, whereas a fluorine atom at C-4 (**52**) abrogates binding to LecA.



We proceeded to perform  $^1\text{H}$ ,  $^{15}\text{N}$ -TROSY experiments with all of the monofluorinated galactosides. The results are shown in Figure 5 in terms of the perturbed backbone resonances upon addition of monofluorinated galactopyranosides **48-55** to LecA.<sup>[38]</sup> Since no assignment of the backbone resonances is available, labelling of the peaks is arbitrary and we utilized these perturbations for fingerprinting the interaction patterns. Similar perturbation patterns would indicate similar binding interactions. Firstly, analogues with fluoro substituents at C-3 (**50**, **51**) and C-4 (**52**, **53**) induced limited chemical shift perturbations or changes in peak intensities, suggesting little or no affinity towards LecA. The hydroxyl groups at C-3 and C-4 of galactose are involved in coordination to the calcium cation bound to LecA.<sup>[39]</sup> Consequently, fluoro substituents at these positions abrogate efficient binding to LecA. For the compounds with a fluoro substituent at C-2 (**48**, **49**) or C-6 (**54**, **55**), marked changes in peak intensity and/or chemical shift were induced. In fact, the largest changes were observed for residues involved in the carbohydrate recognition domain as inferred from galactose binding (Figure 5, top).<sup>[39]</sup> Overall, a consensus of perturbed resonances could be deduced for all of the compounds, suggesting a common binding site (Figure 5, bottom).<sup>[40]</sup>

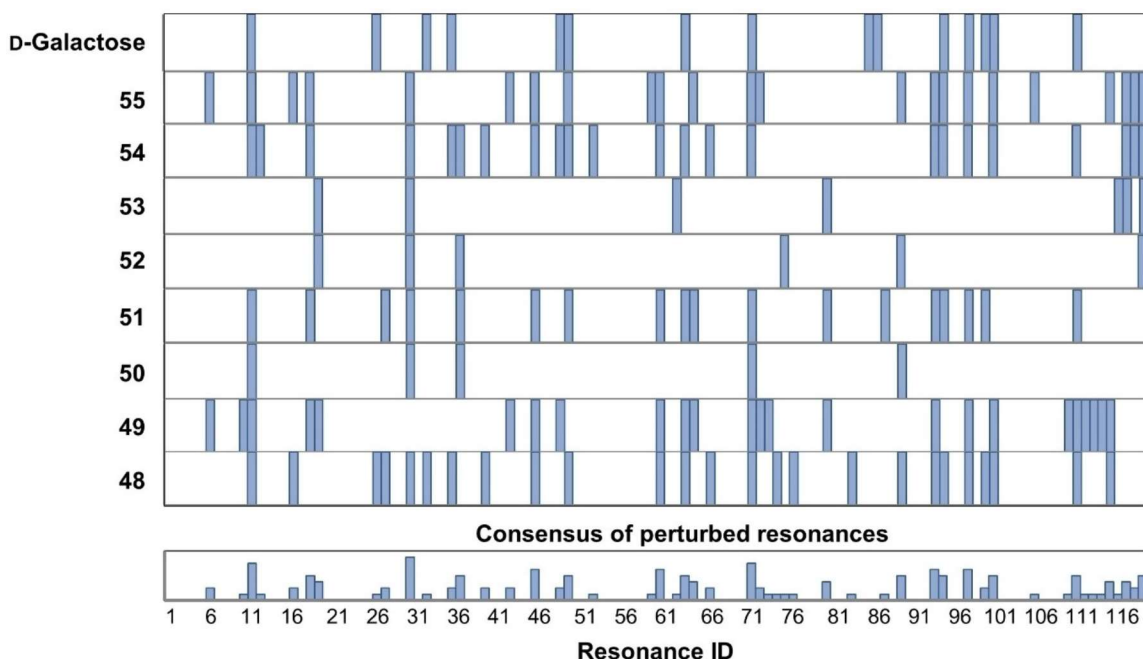


**Figure 5.** Summary of backbone resonances of LecA perturbed by the presence of monofluorinated galactosides (**48-55**) and galactose as observed by  $^1\text{H}$ ,  $^{15}\text{N}$ -TROSY NMR. Resonance IDs are arbitrary and cannot be associated with amino acid residues in the absence of any assignment, but serve as fingerprints to visualize interaction patterns. If the change in peak intensity is more than 20% or if there is a chemical shift perturbation exceeding 0.025 ppm, the residue is highlighted in blue.

Thus far, perturbations of the protein resonances have been used to monitor the interactions. Since the incorporation of a fluorine atom offers exquisite possibilities in NMR, we chose to complement our studies and to take advantage of this by performing  $^{19}\text{F}$  NMR studies of monofluorinated galactoside derivatives in the presence and absence of LecA (Figure 6). Changes in peak intensity in the  $^{19}\text{F}$  NMR spectra were followed, as exemplified for 2-deoxy-2-fluoro-galactopyranoside **48** (Figure 6a). Upon addition of LecA to **48**, broadening of the peak was observed, along with a reduction in its intensity

by about 40%, indicating binding to the lectin. All of the monofluorinated galactopyranosides **48-55** were analyzed analogously (Figure 6b). Taken together, derivatives with a fluoro substituent at C-2 (**48**, **49**) and C-6 (**54**, **55**) showed large changes in peak intensity (35-80%). Among these derivatives, those with the  $\beta$ -S-(2-naphthyl) aglycone (**49**, **55**) showed the largest changes in peak intensity of up to 80%. Finally, although no changes in peak intensity could be observed for compound **50**, significant changes in chemical shift were recorded, indicative of a faster exchange rate on the NMR chemical shift time scale.

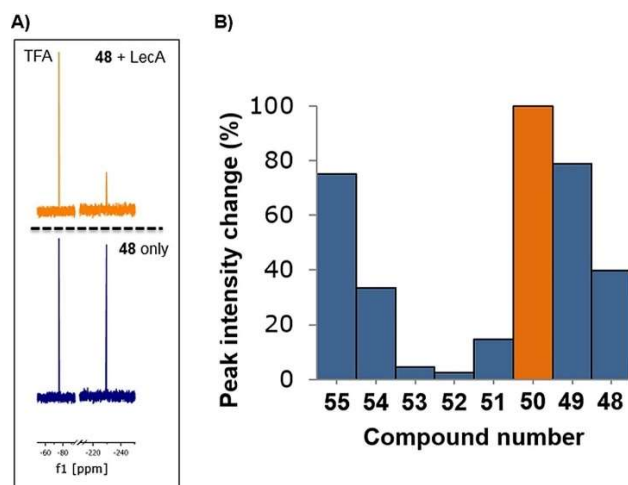


**Figure 6.** Direct observation of <sup>19</sup>F resonances of monofluorinated galactosides upon binding to LecA. A) <sup>19</sup>F NMR spectrum of compound **48** (blue) and in the presence of LecA (orange); reduction of the signal intensity of the galactoside indicates binding to LecA. Both spectra were normalized to reference trifluoroacetic acid (TFA: -75.6 ppm). B) Percent peak intensity changes of <sup>19</sup>F monofluorinated galactosides **48-55** in the presence of LecA (blue) compared to spectra recorded in the absence of LecA. Compound **50** was arbitrarily assigned 100% intensity to indicate binding inferred from chemical shift perturbation (orange) in the absence of intensity reduction.

To evaluate the affinities of the most effective binders, we performed isothermal titration calorimetry experiments on our monofluorinated galactopyranoside analogues (**48**, **49**). A typical thermogram of LecA interacting with compound **49** is given in Figure 7a. Firstly, no binding was observed for the compounds with a fluoro substituent in position 3 or 4, which are involved in coordination to the aforementioned calcium cation. Fluorination at position 2 resulted in a slight decrease in affinity. Fluorination at position 6 had a stronger effect, with decreases of one or two orders of magnitude. This is consistent with the role of each hydroxyl group in the complexation between LecA and galactose (1OKO) (Figure 7b). Oxygen atoms at positions 3 and 4 are crucial for the interaction, being involved in direct coordination of the bridging calcium ion and in hydrogen bonds with amino acid side chains. Oxygen *O*-6 is involved in two direct hydrogen bonds with the protein, and oxygen *O*-2 in only one.

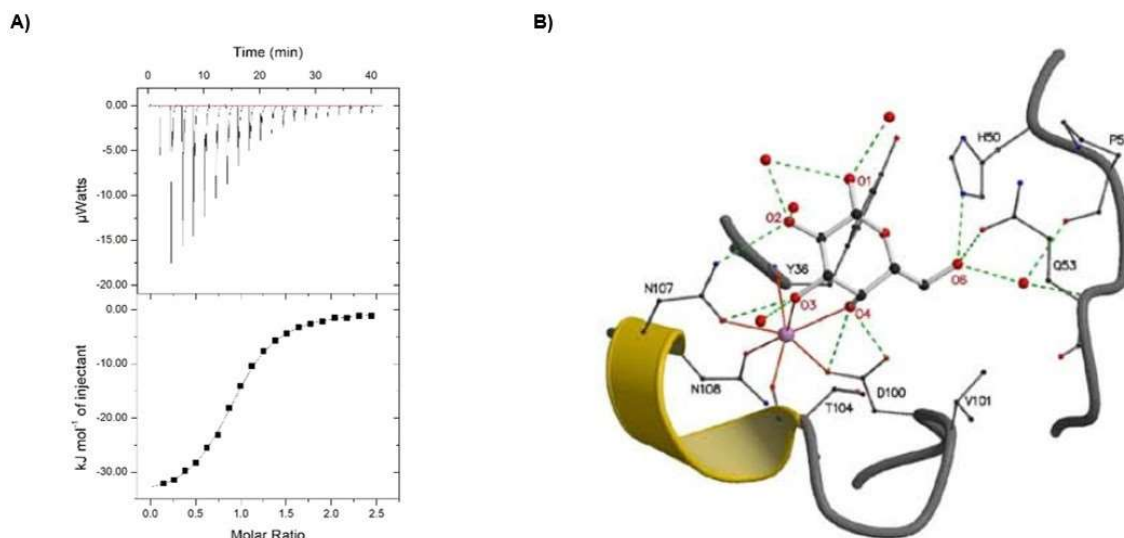


**Figure 7.** A) Thermogram of LecA interacting with compound **49**. The ITC plot (measured by VP-ITC Microcal) in the lower panel shows the total heat released as a function of total ligand concentration for the titration shown in the upper panel. The solid line denotes the best least-squares fit to the experimental data using a one-site model. B) *D*-Galactose in the carbohydrate recognition domain of LecA (1OKO).<sup>[39]</sup>

It was also of interest to evaluate the effect of fluorination on the thermodynamics, by analyzing the enthalpy and entropy contributions of the 2F-derivatives compared to the native compounds. Fluorination at position 2 strongly decreases the enthalpy contribution (loss of 20%), but the entropy barrier is also significantly decreased (Table 3). As a result, the decrease in affinity is limited, corresponding to a loss of about 10% in free energy. The decrease in binding enthalpy can be correlated to the loss of the hydrogen bond to Asn<sub>107</sub>, and the gain in entropy contribution to a modification of the water network. Moreover, as previously observed, the  $\beta$ -S-(2-naphthyl) aglycone (**49**, **55**) provided analogues with higher affinities as compared to their  $\beta$ -*O*-benzoic acid counterparts (**48**, **54**). Furthermore, it is important to point out that compound **49** constitute a privilege class of LecA inhibitor

(three times more potent than methyl  $\beta$ -D-galactopyranose). The aromatic thioglycoside represents a stable functional group in biological media by virtue of the glycosidically stable thio linkage. Not only does the high C-F bond energy render it resistant to *in vivo* degradation, but the fluoro substituent can increase lipophilicity, which in turn can increase cell permeability.<sup>[41]</sup> Finally, in the context of this study, a limitation of our library is the low water solubility of polyfluorinated analogues, especially for compounds with the  $\beta$ -S-(2-naphthyl) aglycone, and the low affinity between fluorine atoms and the calcium cation. One can assume that members of our library of fluorinated analogues would be more suitable as ligands for other galactophilic proteins that do not include a cationic metal center in the carbohydrate recognition domain.

**Table 3.**  $K_d$  values and thermodynamic parameters for the binding of LecA to selected fluorinated galactopyranoside derivatives and reference compounds in ITC assays. Experiments were performed twice and standard deviations were lower than 10%.

Ligand	$-\Delta H^\circ$ [KJ mol <sup>-1</sup> ]	$-T\Delta S^\circ$ [KJ mol <sup>-1</sup> ]	$-\Delta G^\circ$ [KJ mol <sup>-1</sup> ]	$K_d$ [ $\mu$ M]
$\alpha$ -Gal- <i>O</i> -Me	40.9	16.3	24.6	50.0
$\beta$ -Gal- <i>O</i> -Me	19.0	5.3	24.3	55.7
$\beta$ -Gal- <i>O</i> - <i>p</i> -benzoic acid	38.9	11.1	27.8	13.0
$\beta$ -Gal- <i>S</i> -2-thionaphthyl	45.1	14.8	30.3	4.8
<b>48</b>	31.9	6.9	25.0	41
<b>49</b>	35.3	8.1	27.2	17
<b>54<sup>a</sup></b>	32.7	12.6	20.1	303
<b>55<sup>a</sup></b>	27.4	5.2	22.3	124.2

<sup>a</sup>Due to low affinity, a sigmoid curve could not be obtained for compounds **54** and **55**, which precluded the determination of reliable DH values.

## Conclusions

The preparation and characterization of the first library of fluorinated galactopyranosides has been achieved, with two aglycones at the anomeric position:  $\beta$ -*O*-benzoic acid and  $\beta$ -*S*-(2-naphthyl). Most of the fluorinated compounds showed no antiproliferative activity against normal or cancer cell lines. Our library of stable glycomimetics could be used as molecular probes towards galactophilic lectins. The first TROSY NMR analyses of chemical shift perturbations of LecA, as well as  $^{19}\text{F}$  NMR studies in the presence and absence of LecA, suggested that analogues with fluoro substituents at C-3 or C-4 have low affinities for LecA. Compounds with fluoro substituents at C-2 and C-6, however, showed strong changes in peak intensity or chemical shift perturbations. These results were corroborated by isothermal titration calorimetry experiments. Compound **49** was identified as a high-affinity ligand for LecA, with a dissociation constant of 17  $\mu\text{M}$ . The present investigation clearly shows the importance of systematic investigations in the search for stable and potent glycomimetics as lectin ligands. By combining organic synthesis and biological studies, we strongly believe that the resulting molecules could serve as useful tools to expedite the use of stable glycomimetics. This should underscore their relevance, and their hitherto underestimated potential in medicine.

## Experimental Section

### Chemical synthesis

All reactions were carried out under an argon atmosphere with dry solvents under anhydrous conditions, unless otherwise noted. Dry tetrahydrofuran (THF), toluene, benzene, diethyl ether ( $\text{Et}_2\text{O}$ ), *N,N*-dimethylformamide (DMF), and dichloromethane

(CH<sub>2</sub>Cl<sub>2</sub>) were obtained by passing commercially available pre-dried, oxygen-free formulations through activated alumina columns. Yields refer to chromatographically and spectroscopically (NMR) homogeneous materials, unless otherwise stated. Reagents were purchased at the highest commercial quality and used without further purification, unless otherwise stated. Reactions were monitored by thin-layer chromatography (TLC) carried out on 200 μm SiliaPlate aluminium-backed plates (indicator F-254) using UV light for visualization and an ethanolic solution of phenol and sulfuric acid and heat as developing agents. SiliaFlash P60 (particle size 40-63 μm, 230-400 mesh) was used for flash column chromatography. NMR spectra were recorded on an Agilent DD2 spectrometer (at 500 MHz for <sup>1</sup>H, 470 MHz for <sup>19</sup>F, and 126 MHz for <sup>13</sup>C) and calibrated using residual undeuterated solvent peaks (chloroform-*d*: δ<sub>H</sub>=7.26 ppm, δ<sub>C</sub>=77.16 ppm; [D<sub>6</sub>]DMSO: δ<sub>H</sub>=2.50 ppm, δ<sub>C</sub>=39.52 ppm; [D<sub>6</sub>]acetone: δ<sub>H</sub>=2.05 ppm, δ<sub>C</sub>=29.84 ppm; methanol-*d*<sub>4</sub>: δ<sub>H</sub>=3.31 ppm, δ<sub>C</sub>=49.0 ppm) as an internal reference. <sup>19</sup>F NMR spectra were calibrated using hexafluorobenzene, which gives a signal at δ<sub>F</sub>=-162.29 ppm with respect to that of the reference compound CFC<sub>3</sub>. The following abbreviations are used to designate multiplicities: s=singlet, d=doublet, t=triplet, q=quartet, p=quintet, h=sextet, m=multiplet, br=broad. Infrared (IR) spectra were recorded on a Thermo Nicolet 380 FTIR spectrometer, with a ZnSe crystal plate. High-resolution mass spectra (HRMS) were recorded on an Agilent series 1200 TOF (time-of-flight) 6210 mass spectrometer in ESI (electrospray ionization) mode. Melting points were recorded on a Stanford Research Systems Optimelt MPA100 automated melting point system and are uncorrected. Optical rotations were recorded on a JASCO DIP-360 digital polarimeter at 589 nm, and are reported in units of 10<sup>-1</sup> (deg cm<sup>-2</sup> g<sup>-1</sup>).



## Cell lines culture

HaCaT primary epidermal keratinocyte and human HDFn neonatal dermal fibroblast cells were purchased from Thermo-Fisher Scientific. Mouse 3T3 embryonic fibroblast and human HT-29 colon adenocarcinoma cells were purchased from the American Type Culture Collection (Manassas, VA). M21 human skin melanoma cells were kindly provided by Dr. David Cheresch (University of California, San Diego School of Medicine). HaCaT and 3T3 cells were cultured in high-glucose Dulbecco's minimal essential medium (DMEM, Gibco, Thermo-Fisher Scientific) supplemented with 10% (v/v) fetal bovine serum (FBS, Gibco, Thermo-Fisher Scientific) and 1% antibiotic penicillin-streptomycin (5,000 U mL<sup>-1</sup>). HDFn cells were cultured in DMEM supplemented with 2% (v/v) FBS, 1% penicillin-streptomycin, fibroblast growth factor (3 ng mL<sup>-1</sup>), epidermal growth factor (10 ng mL<sup>-1</sup>), hydrocortisone (1 ng mL<sup>-1</sup>), and heparin (10 ng mL<sup>-1</sup>). HT-29 and M21 cells were cultured in DMEM supplemented with 5% FBS. Cells were maintained at 37 °C in a moisture-saturated atmosphere containing 5% CO<sub>2</sub>.

## Antiproliferative activity assay

The growth inhibition potencies of all of the compounds were assessed using the procedure recommended by the National Cancer Institute (NCI) Developmental Therapeutics Program for its drug screening program, with slight modifications.<sup>[42]</sup> Briefly, 96-well Costar microtiter clear plates were seeded with 75  $\mu$ L of a suspension of either HaCaT (4.5x10<sup>3</sup>), 3T3 (3x10<sup>3</sup>), HDFn (3x10<sup>3</sup>), HT-29 (5x10<sup>3</sup>), or M21 (3x10<sup>3</sup> cells per well) in the appropriate medium. Plates were incubated for 24 h. Freshly solubilized drugs in DMSO (40 mM) were diluted with fresh medium, and 75  $\mu$ L aliquots containing serially

diluted concentrations of the drug were added. The final drug concentrations ranged from 100  $\mu\text{M}$  to 78 nM. The DMSO concentration was kept constant at <0.5% (v/v) to prevent any related toxicity. Plates were incubated for 48 h, after which growth was stopped by the addition of cold trichloroacetic acid to the wells (final concentration 10% w/v). The plates were then incubated at 4 °C for 1 h. They were then washed five times with distilled water and a sulforhodamine B solution (0.1 %, w/v) in 1% acetic acid was added to each well. After 15 min at room temperature, the excess dye was removed and the plates were washed five times with 1% aqueous acetic acid. Bound dye was solubilized in 20 mM Tris base and the absorbance was read in the optimal wavelength range of 530-580 nm with a SpectraMax i3x (Molecular Devices). Data obtained from treated cells were compared to those from control cell plates fixed on the treatment day, allowing the percentage of cell growth to be calculated for each drug. The experiments were performed at least twice in triplicate. The assays were considered valid when the coefficient of variation was <10% for a given set of conditions within the same experiment.

### **$^1\text{H},^{15}\text{N}$ TROSY NMR**

Fluorinated galactopyranoside binding to LecA was assessed through protein-observed  $^1\text{H},^{15}\text{N}$  TROSY NMR. All  $^1\text{H},^{15}\text{N}$  TROSY measurements were performed at 310 K with samples in Norell S-3-800-7 3 mm tubes on a Bruker Ascend 700 MHz spectrometer (Bruker, Billerica, MA, USA) equipped with a 5 mm TCI700 CryoProbe.

Briefly,  $^1\text{H},^{15}\text{N}$  TROSY spectra of 350  $\mu\text{M}$  ( $U\text{-}^{15}\text{N}$ ) LecA were recorded from solutions in 20 mM HEPES, 150 mM NaCl, pH 7.4 buffer containing 10 mM  $\text{CaCl}_2$ , 100  $\mu\text{M}$  DSS as internal reference, and 10%  $\text{D}_2\text{O}$ . Each fluorinated  $\text{D}$ -galactose compound (0.2-1.5 mM) in

[D<sub>6</sub>]DMSO was added and the obtained spectrum was compared to that acquired with the same amount (v/v) of [D<sub>6</sub>]DMSO to factor out changes caused by the solvent. A <sup>1</sup>H, <sup>15</sup>N TROSY pulse sequence with WATERGATE solvent suppression, 128 increments, and 16 scans per increment was applied. Data were processed with NMRpipe<sup>[43]</sup> and further analyzed with CCPN.<sup>[44]</sup>

<sup>1</sup>H, <sup>15</sup>N TROSY resonances were indexed with IDs from 1 to 118 due to a lack of protein backbone resonance assignment. Based on this reference spectrum, resonance IDs were transferred to the spectrum obtained in the presence of the compound in order to compare the changes. In the case of ambiguities caused by strongly overlapping or disappearing peaks between the spectra, resonance IDs were not transferred. Chemical shift perturbations (CSPs) were calculated according to Equation (1):

$$\Delta\delta = \sqrt{\frac{1}{2}[\Delta\delta_{\text{H}}^2 + (a\Delta\delta_{\text{N}})^2]}$$

in which  $\Delta\delta_i$  is the difference in chemical shift (in ppm) and  $a$  is an empirical weighting factor of 0.14 for all amino acid backbone resonances.<sup>[45]</sup> The threshold value was set at 0.015 ppm based on four independent measurements of reference spectra. In addition to CSPs, peaks incurring a loss in normalized signal intensity of 20% or more compared to the reference spectrum were taken as indicators of carbohydrate binding.

### **<sup>19</sup>F NMR measurements**

Ligand-observed <sup>19</sup>F NMR was performed to validate binding of fluorinated galactopyranosides to LecA. Briefly, spectra of 50 μM of the compound in the absence and

presence of 100  $\mu\text{M}$  LecA in TBS buffer (25 mM Tris, 150 mM NaCl, pH 7.8, 10 mM  $\text{CaCl}_2$ , 100  $\mu\text{M}$  TFA, 10%  $\text{D}_2\text{O}$ ) were recorded at 310 K from solutions in Norell S-3-800-7 3 mm tubes on a Bruker Ascend 700 MHz spectrometer (Bruker, Billerica, MA, USA) equipped with a 5 mm TCI700 CryoProbe. All spectra were normalized to the signal of the internal reference TFA at  $\delta = -75.6$  ppm and analyzed for changes in peak intensity or chemical shift. Compounds were assigned as binding LecA in  $^{19}\text{F}$  NMR experiments when their combination elicited changes in peak intensity of more than 20% or a chemical shift difference of 0.025 ppm or more.

### **Isothermal titration calorimetry**

Recombinant lyophilized LecA was dissolved in buffer (20 mM Tris-HCl, 100  $\mu\text{M}$   $\text{CaCl}_2$ , 100 mM NaCl, pH 7.5) and the solution was degassed. The protein concentration (50-300  $\mu\text{M}$ ) was assessed by measuring the optical density, assuming a theoretical molar extinction coefficient of 28000. Galactose derivatives were directly dissolved in the same buffer, and the solutions were degassed and placed in the injection syringe (concentrations varying from 1.3 to 1.5 mM). ITC was performed using an ITC-200 microcalorimeter (MicroCal Inc). LecA was placed in the 200  $\mu\text{M}$  sample cell at 25  $^\circ\text{C}$ . Titrations were performed by injecting aliquots (2  $\mu\text{L}$ ) of carbohydrate ligand solutions at intervals of 120 s. Data were fitted according to the “one-site model” using MicroCal Origin 7 software according to standard procedures. Fitted data yielded the stoichiometry ( $n$ ), the association constant ( $K_a$ ), and the enthalpy of binding ( $\Delta H$ ). Other thermodynamic parameters (i.e., changes in free energy  $\Delta G$  and entropy  $\Delta S$ ) were calculated from the equation  $\Delta G = \Delta H -$

$T\Delta S = -RT \ln Ka$ , where T is the absolute temperature and  $R = 8.314 \text{ J mol}^{-1} \text{ K}^{-1}$ . Two or three independent titrations were performed for each ligand tested.

### Acknowledgements

This work was supported by the Natural Sciences and Engineering Research Council of Canada (NSERC), the Fonds de Recherche du Québec—Nature et Technologies, CHU de Québec-Université Laval Research Center, and the Université Laval. D.L. thanks the Fonds de Recherche du Québec—Nature et Technologies for a postgraduate fellowship. We thank Pierre Audet for NMR assistance (Université Laval) and Thierry Marris for crystallographic assistance (Université de Montréal). This work has been partially supported by Glyco@Alps project (ANR-15-IDEX-02), Labex ARCANE, GLYCOMIME (ANR-17-CE11-0048), and CBH-EUR-GS (ANR-17-EURE-0003). Finally, the authors would like to thank Dr. Yoann M. Chabre for useful discussions.

### Conflict of interest

The authors declare no conflict of interest.

### References

- [1] a) S. M. Ametamey, M. Honer, P. A. Schubiger, *Chem. Rev.* **2008**, 108, 1501-1516; b) S. Preshlock, M. Tredwell, G. Gouverneur, *Chem. Rev.* **2016**, 116, 719-766; c) H. H. Coenen, P. H. Elsinga, R. Iwata, M. R. Kilbourn, M. R. A. Pillai, M. G. R. Rajan, H. N. Wagner, J. J. Zaknum, *Nucl. Med. Biol.* **2010**, 37, 727-740; d) D. A. Mankoff, F. Dehdashti, A. F. Shields, *Neoplasia* **2000**, 2, 71-88.

- [2] a) “Fluorinated sugars as probes of glycosidase mechanism”: M. Namchuk, C. Braun, J. D. McCarter, S. G. Withers, in *ACS Symposium Series, Vol. 639* (Eds.: I. Ojima, J. McCarthy, J. T. Welch), American Chemical Society, Washington, DC, **1996**, pp. 279-293; b) S. J. Williams, S. G. Withers, *Carbohydr. Res.* **2000**, 327, 27-46; c) S. A. Allam, H. H. Jensen, B. Vijaykrishnan, J. A. Garnett, E. Leon, Y. Liu, D. C. Anthony, N. R. Sibson, T. Feizi, S. Matthews, B. G. Davis, *ChemBioChem* **2009**, 10, 2522-2529.
- [3] H. Lis, N. Sharon, *Chem. Rev.* **1998**, 98, 637-674.
- [4] A. Varki, R. Cummings, J. Esko, H. Freeze, G. Hart, J. Marth, *Essentials of Glycobiology*, Cold Spring Harbor Laboratory Press, Cold Spring Harbor, **1999**.
- [5] T. K. Dam, F. C. Brewer, *Chem. Rev.* 2002, 102, 387-429.
- [6] *Subcellular Biochemistry Vol. 32:  $\alpha$ -Gal and anti-Gal:  $\alpha$ -1,3-galactosyltransferase,  $\alpha$ -Gal epitopes, and the natural anti-Gal antibody* (Eds.: U. Galili, J. L. Avila), Kluwer, New York, 1999, p. 394.
- [7] a) “ $\beta$ -Galactoside-binding vertebrate lectins: synthesis, molecular biology, function”: R. Lotan, in *Glycoconjugates* (Eds.: H. J. Allen, E. C. Kisailus), Marcel Dekker, New York, **1992**, pp. 635-671; b) J. T. Powell, F. L. Harrison, *Am. J. Physiol.* **1991**, 261, L236-L239; c) K. Kasai, *Adv. Lectin Res.* **1990**, 3, 10-35; d) M. Caron, D. Bladier, R. Joubert, *Int. J. Biochem.* **1990**, 22, 1379-1385; e) A. M. Wu, S. Sugii, *Adv. Exp. Med. Biol.* **1988**, 228, 505-263.

- [8] a) A. Imberty, Y. M. Chabre, R. Roy, *Chem. Eur. J.* **2008**, 14, 7490-7499; b) L. Bhattacharyya, F. C. Brewer, *Eur. J. Biochem.* **1988**, 176, 207-212.
- [9] O. Hindsgaul, T. Norberg, J. Le Pendu, R. U. Lemieux, *Carbohydr. Res.* **1982**, 109, 109-142.
- [10] T. Diercks, A. S. Infantino, L.Unione, J. Jim8nez-Barbero, S. Oscarson, H.-J. Gabius, *Chem. Eur. J.* **2018**, 24, 15761-15765.
- [11] M. Hoffmann, J. Rychlewski, *Int. J. Quantum Chem.* **2002**, 89, 419-427.
- [12] M. Reindl, A. Hoffmann-Rçder, *Curr. Top. Chem.* **2014**, 14, 840-854.
- [13] a) H. J. Bçhm, D. Banner, S. Bendels, M. Kansy, B. Kuhn, K. Meller, U. Obst-Sander, M. Stahl, *ChemBioChem* **2004**, 5, 637-643; b) S. Purser, P. R. Moore, S. Swallow, V. Gouverneur, *Chem. Soc. Rev.* **2008**, 37, 320-330; c) E. P. Gillis, K. J. Eastman, M. D. Hill, D. J. Donnelly, N. A. Meanwell, *J. Med. Chem.* **2015**, 58, 8315-8359.
- [14] a) V. Denavit, D. Lain8, J. St-Gelais, P. A. Johnson, D. GiguHre, *Nat. Commun.* **2018**, 9, 4721; b) D. Lain8, V. Denavit, D. GiguHre, *J. Org. Chem.* **2017**, 82, 4986-4992; c) "Fluorine-containing carbohydrates: synthesis of 6-deoxy-6-fluoro-1,2:3,4-di-O-isopropylidene- $\alpha$ -D-galactopyranose": V. Denavit, D. Lain8, G. Le Heiget, D. GiguHre, in *Carbohydrate Chemistry: Proven Synthetic Methods, Vol. 4* (Eds.: C. Vogel, P. V. Murphy), Wiley-VCH, Weinheim, **2017**, Chap. 30, pp. 241-246.

- [15] a) D. GiguHre, S. Sato, C. St-Pierre, S. Sirois, R. Roy, *Bioorg. Med. Chem. Lett.* **2006**, *16*, 1668-1672; b) J. Rodrigue, G. Ganne, B. Blanchard, C. Saucier, D. GiguHre, T. C. Shiao, A. Varrot, A. Imberty, R. Roy, *Org. Biomol. Chem.* **2013**, *11*, 6906-6918; c) J. C. D. Arribas, A. G. Herrero, M. Martin-Lomas, F. J. Canada, S. He, S. G. Withers, *Eur. J. Biochem.* **2000**, *267*, 6996-7005.
- [16] a) S. G. Withers, M. D. Percival, I. P. Street, *Carbohydr. Res.* **1989**, *187*, 43-66; b) B. P. Rempel, S. G. Withers, *Aust. J. Chem.* **2009**, *62*, 590-599; c) J.-S. Zhu, N. E. McCormick, S. C. Timmons, D. L. Jakeman, *J. Org. Chem.* **2016**, *81*, 8816-8825.
- [17] a) I. P. Street, C. R. Armstrong, S. G. Withers, *Biochemistry* **1986**, *25*, 6021-6027; b) H. W. Kim, P. Rossi, R. K. Shoemaker, S. G. DiMagno, *J. Am. Chem. Soc.* **1998**, *120*, 9082-9083; c) I. N'Go, S. Golten, A. Arda, J. Canada, J. Jimenez-Barbero, B. Linclau, S. P. Vincent, *Chem. Eur. J.* **2014**, *20*, 106-112; d) K. E. van Straaten, J. R. A. Kuttiyatveetil, C. M. Sevrain, S. A. Villaume, J. Jimenez-Barbero, B. Linclau, S. P. Vincent, D. A. R. Sanders, *J. Am. Chem. Soc.* **2015**, *137*, 1230-1244.
- [18] a) T. Oberbillig, C. Mersch, S. Wagner, A. Hoffmann-Rçder, *Chem. Commun.* **2012**, *48*, 1487-1489; b) A. Baumann, S. Marchner, M. Daum, A. Hoffmann-Rçder, *Eur. J. Org. Chem.* **2018**, 3803-3815.
- [19] a) S. Bresciani, T. Lebl, A. M. Z. Slawin, D. O'Hagan, *Chem. Commun.* **2010**, *46*, 5434-5436; b) J. C. Biffinger, H. W. Kim, S. G. DiMagno, *ChemBioChem* **2004**, *5*, 622-627.



- [20] a) J. A. Olsen, D. W. Banner, P. Seiler, U. Obst-Sander, A. D'Arcy, M. Stihle, K. Muller, F. Diederich, *Angew. Chem. Int. Ed.* **2003**, *42*, 2507-2511; *Angew. Chem.* **2003**, *115*, 2611-2615; b) R. Paulini, K. Muller, F. Diederich, *Angew. Chem. Int. Ed.* **2005**, *44*, 1788-1805; *Angew. Chem.* **2005**, *117*, 1820-1839; c) K. Muller, C. Faeh, F. Diederich, *Science* **2007**, *317*, 1881-1886.
- [21] J. D. McCarter, M. J. Adam, S. G. Withers, *Biochem. J.* **1992**, *286*, 721-727.
- [22] a) A. G. Watts, P. Oppezzo, S. G. Withers, P. M. Alzari, A. Buschiazzo, *J. Biol. Chem.* **2006**, *281*, 4149-4155; b) M. N. Namchuk, J. D. McCarter, A. Becalski, T. Andrews, S. G. Withers, *J. Am. Chem. Soc.* **2000**, *122*, 1270-1277; c) S. G. Withers, K. Rupitz, I. P. Street, *J. Biol. Chem.* **1988**, *263*, 7929-7932; d) S. G. Withers, I. P. Street, D. H. Dolphin, *J. Am. Chem. Soc.* **1987**, *109*, 7530-7531.
- [23] a) M. C. Kasuya, A. Ito, K. Hatanaka, *J. Fluorine Chem.* **2007**, *128*, 562-565; b) J. Ortner, M. Albert, H. Weber, K. Dax, *J. Carbohydr. Chem.* **1999**, *18*, 297-316.
- [24] See the Supporting Information for more details.
- [25] a) M. Cerny, J. Stanek, *Adv. Carbohydr. Chem. Biochem.* **1977**, *34*, 23-178; b) M. Cerny, O. Julakova, J. Pacak, *Collect. Czech. Chem. Commun.* **1974**, *39*, 1391-1396.
- [26] a) R. Lattrell, G. Lohaus, *Justus Liebigs Ann. Chem.* **1974**, 901-920; b) R. Albert, K. Dax, R. W. Link, A. E. Stutz, *Carbohydr. Res.* **1983**, *118*, C5-C6.
- [27] T. B. Grindley, R. Thangarasa, *Carbohydr. Res.* **1988**, *172*, 311-318.
- [28] T. Trnka, M. Cerny, *Collect. Czech. Chem. Commun.* **1971**, *36*, 2216-2225.

- [29] S. Hornik, L.C. Stastna, P. Curinova, J. Sykora, K. Kanova, R. Hrstka, M. Dracinsky, J. Karban, *Beilstein J. Org. Chem.* **2016**, *12*, 750-759.
- [30] P. Sarda, F. C. Escribano, R. J. Alves, A. Olesker, G. Lukacs, *J. Carbohydr. Chem.* **1989**, *8*, 115-123.
- [31] P.-O. Lin, A. K. Adak, S.-H. Ueng, L.-D. Huang, K.-T. Huang, J.-A. A. Ho, C.-C. Lin, *J. Org. Chem.* **2009**, *74*, 4041-4048.
- [32] CCDC 1824899 (**57**) contains the supplementary crystallographic data for this paper. These data can be obtained free of charge from The Cambridge Crystallographic Data Centre.
- [33] CCDC 1848261 (**57**) contains the supplementary crystallographic data for this paper. These data can be obtained free of charge from The Cambridge Crystallographic Data Centre.
- [34] K. Bock, J. O. Duus, *J. Carbohydr. Chem.* **1994**, *13*, 513-543.
- [35] L. B. Rice, *J. Infect. Dis.* **2008**, *197*, 1079-10881.
- [36] C. Chemani, A. Imberty, S. de Bentzman, M. Pierre, M. Wimmerova, B. P. Guery, K. Faure, *Infect. Immun.* **2009**, *77*, 2065-2075.
- [37] a) N. Garber, U. Guempel, A. Belz, N. Gilboa-Garber, R. J. Doyle, *Biochim. Biophys. Acta* **1992**, *1116*, 331-333; b) R. U. Kadam, M. Bergmann, M. Hurley, D. Garg, M. Cacciarini, M. A. Swiderska, C. Nativi, M. Sattler, A. R. Smyth, P. Williams, M. Camara, A. Stocker, T. Darbre, J.-L. Reymond, *Angew. Chem. Int. Ed.* **2011**, *50*,

10631-10635; *Angew. Chem.* **2011**, 123, 10819-10823; c) I. Otsuka, B. Blanchard, R. Borsali, A. Imberty, T. Kakuchi, *ChemBioChem* **2010**, 11, 2399-2408.

- [38] For a more detailed account of the chemical shift perturbation, see the Supporting Information.
- [39] a) G. Cioci, E. P. Mitchell, C. Gautier, M. Wimmerova, D. Sudakevitz, S. Perez, N. Gilboa-Garber, A. Imberty, *FEBS Lett.* **2003**, 555, 297-301.
- [40] S. Wagner, D. Hauck, M. Hoffmann, R. Sommer, I. Joachim, R. Muller, A. Imberty, A. Varrot, A. Titz, *Angew. Chem. Int. Ed.* **2017**, 56, 16559-16564; *Angew. Chem.* **2017**, 129, 16786-16791.
- [41] B. Linclau, Z. Wang, G. Compain, V. Paumelle, C. Q. Tontenelle, N. Wells, A. Weymouth-Wilson, *Angew. Chem. Int. Ed.* **2016**, 55, 674-678; *Angew. Chem.* **2016**, 128, 684-688.
- [42] Developmental therapeutics program human tumor cell line screen, National Cancer Institute (NCI/NIH), [https://dtp.cancer.gov/discovery\\_development/nci-60/default.htm](https://dtp.cancer.gov/discovery_development/nci-60/default.htm), accessed February 21, 2018.
- [43] F. Delaglio, S. Grzesiek, G. Vuister, G. Zhu, J. Pfeifer, A. Bax, *J. Biomol. NMR* **1995**, 6, 277-293.
- [44] W. F. Vranken, W. Boucher, T. J. Stevens, R. H. Fogh, A. Pajon, M. Llinas, E. L. Ulrich, J. L. Markley, J. Ionides, E. D. Laue, *Proteins Struct. Funct. Bioinf.* **2005**, 59, 687-696.

[45] M. P. Williamson, *Prog. Nucl. Magn. Reson. Spectrosc.* **2013**, 73, 1-16.